International Journal of Pharmaceutics 387 (2010) 34–41

Contents lists available at ScienceDirect

International Journal of Pharmaceutics

journal homepage: www.elsevier.com/locate/ijpharm

Characterization of two blood–brain barrier mimicking cell lines: Distribution of lectin-binding sites and perspectives for drug delivery

V.E. Plattner[a], B. Germann[b], W. Neuhaus[c], C.R. Noe[b], F. Gabor[a], M. Wirth[a,*]

[a] Department of Pharmaceutical Technology and Biopharmaceutics, University of Vienna, A-1090 Vienna, Austria
[b] Department of Medicinal Chemistry, University of Vienna, A-1090 Vienna, Austria
[c] PharmaCon GmbH, Riglergasse 4/5, A-1180 Vienna, Austria

ARTICLE INFO

Article history:
Received 15 May 2009
Accepted 28 November 2009
Available online 4 December 2009

Keywords:
Blood–brain barrier
ECV304
PBMEC/C1–2
Lectins
Drug targeting

ABSTRACT

In the present study plant lectins with distinct sugar specificities were applied to two blood–brain barrier (BBB) mimicking cell lines, namely human ECV304 and porcine brain microvascular endothelial cells PBMEC/C1–2 in order to elucidate their glycosylation pattern and to evaluate the lectin-cell interaction for lectin-mediated targeting. The bioadhesive properties of fluorescein-labeled lectins were investigated with monolayers as well as single cells using fluorimetry and flow cytometry, followed by confirmation of the specificity of binding. For PBMEC/C1–2 layers highest binding capacity was found for wheat germ agglutinin (WGA), followed by *Dolichus biflorus* agglutinin (DBA) whereas single cell experiments revealed a predominance of DBA only. Analyzing ECV304 monolayers and single cells, WGA yielded the strongest interaction without any changes during cultivation. The binding capacities of the other lectins increased significantly during differentiation. As similar results to primary cells and brain sections were observed, both cell lines seem to be suitable as models for lectin-interaction studies. Thus, an additional focus was set on the mechanisms involved in uptake and intracellular fate of selected lectins. Cytoinvasion studies were performed with WGA for human ECV304 cells and WGA as well as DBA for PBMEC/C1–2 cells. For both lectins, the association rate to the cells was dependent on temperature which indicated cellular uptake.

1. Introduction

Unlike peripheral endothelium, brain microvascular endothelial cells (BMEC) are characterized by minimal pinocytotic activity, the absence of fenestrations and the presence of tight intercellular junctions (Joo, 1996). They are the main components of the blood–brain barrier (BBB) which maintains the homeostasis of the brain microenvironment and strongly restricts the transport of many drugs from blood to brain.

The surface of the BMECs is covered by a dense layer of complex carbohydrates collectively known as the "glycocalyx" which is thought to contribute to the barrier function (Vorbrodt et al., 1986; Fatehi et al., 1987; Nico et al., 1998). Biorecognitive proteins such as lectins are capable of detecting and binding to these carbohydrate moieties at the cell surface by a highly specific interaction. Consequently, lectins may serve as a tool for analysis of the carbohydrate composition of the glycocalyx. Additionally, several studies have outlined the perspectives of lectin-mediated drug delivery (Lehr, 2000; Gabor and Wirth, 2003; Naeem et al., 2007) including glycotargeting of the BBB (Fischer and Kissel, 2001; Bies et al., 2004).

As investigation of the blood–brain barrier and its function *in vivo* is a challenging task, *in vitro* models mimicking blood–brain barrier characteristics are useful tools for preliminary studies. Primary brain endothelial cells seem to retain more properties of the original tissue, but cultivation is time-consuming and cells have a limited lifespan. Thus, particularly for drug delivery studies cell culture models are preferred as the phenotypic characteristics are stable over a long period including good reproducibility of data. Moreover, cultures of cell lines can easily be cultivated and expanded at will which reduces cost and labor (Cucullo et al., 2005). For that reason, two of the most promising BBB mimicking cell lines, namely human ECV304 and porcine PBMEC/C1–2, were chosen for systematic characterization of the lectin-binding pattern at the monolayer and single cell level. The ECV304 cell line was introduced by Takahashi et al. (1990) and recommended in a previous study to be suitable for BBB drug transport studies (Garberg et al., 2005; Neuhaus et al., 2008a). The cell line PBMEC/C1–2 was established by Teifel and Friedl (Teifel and Friedl, 1996) and used as an *in vitro* model of the BBB in several studies (Vanier et al., 2004, 2006; Neuhaus et al., 2008c). Both cell lines were cultured in astrocyte conditioned medium (ACM) in order to induce typical BBB proper-

* Corresponding author. Tel.: +43 1 4277 55407; fax: +43 1 4277 9554.
E-mail address: michael.wirth@univie.ac.at (M. Wirth).

0378-5173/$ – see front matter © 2009 Elsevier B.V. All rights reserved.
doi:10.1016/j.ijpharm.2009.11.030

ties (Janzer and Raff, 1987; Easton and Abbott, 2002; Neuhaus et al., 2008a,b).

The aim of this study was to assess the binding characteristics and binding specificities of several plant lectins with distinct carbohydrate combining sites on these cell lines. To cover a broad range of sugar structures at the cell surface, lectins were chosen as follows: wheat germ agglutinin (WGA), *Solanum tuberosum* lectin (STL), *Lens culinaris* agglutinin (LCA), *Ulex europaeus* isoagglutinin I (UEA-I), *Dolichus biflorus* agglutinin (DBA) and peanut agglutinin (PNA). Ongoing from these results, an estimation of the glycosylation pattern of cell lines ECV304 and PBMEC/C1–2 and their feasibility as BBB models for elucidation of lectin-mediated drug delivery should be possible. An additional focus was set on the mechanisms involved in uptake and intracellular fate of selected lectins as beneficial for targeted drug delivery.

2. Materials and methods

2.1. Materials

Isocove's modified Dulbecco's medium (IMDM), Ham's F12, Newborn calf serum (NCS), L-Glutamine, Penicillin/Streptomycin and Trypsin/EDTA were bought from Invitrogen Corporation (Gibco™, CA, USA). Transferrin, Amphotericin B and Gelatine were purchased from Sigma (MO, USA). Heparin was obtained from Fluka (Buchs, Switzerland). Cell culture flasks and 96-well plates were bought from Greiner Bio-one (Kremsmünster, Austria).

Fluorescein-labeled WGA (molar ratio fluorescein/protein (F/P) = 2.9), STL (F/P = 3.1), LCA (F/P = 3.8), UEA-I (F/P = 2.7), DBA (F/P = 2.2) and PNA (F/P = 5.2) were purchased from Vector laboratories (Burlingame, USA) and contained >98% active conjugate and no free fluorescein.

2.2. Cell culture

Cell line C6 derived from a rat glioma (Benda et al., 1968) was used in order to produce ACM. They were obtained from the German Cancer Research Center Heidelberg (DKFZ, Heidelberg, Germany) and cultured in C6 medium. The C6 medium is a 1:1 mixture of Ham's F12 and IMDM supplemented with 7.5% (v/v) new born calf serum (NCS), 7 mM L-Glutamine, 5 μg/ml Transferrin, 0.5 U/ml Heparin, 100 U/ml penicillin, 100 μg/ml Streptomycin and 0.25 μg/ml Amphotericin B. In order to obtain ACM the supernatant of a C6 culture was collected every other day.

PBMEC/C1–2 cells were a kind gift from Teifel and Friedl (Teifel and Friedl, 1996) and cultured in PBMEC medium (50% C6 medium, 50% ACM).

The ECV304 cell line was purchased from the European Collection of Animal Cell Cultures (ECACC, Wiltshire, UK) and also maintained in PBMEC medium. For single cell studies cells were seeded on gelatine-coated culture flasks and grown to confluence. Cells were harvested by trypsination, centrifuged (1000 × *g*, 4 °C, 10 min) and resuspended in PBMEC medium at a concentration of 6×10^6 cells/ml. For monolayer studies cells were seeded on gelatine-coated 96-well plates at a concentration of 8×10^4 cells/cm^2 and grown to confluence. Lectin-interaction studies were carried out on day 4 with both cell lines and additionally on day 14 with ECV304 cells only. All cells were cultured at 37 °C, 5% CO_2 and 96% humidity.

2.3. Cytoadhesion studies

Lectin binding was investigated using both monolayers and single cells. Monolayers cultivated in 96-well plates were washed twice with 150 μl PBS per well prior to incubation with 50 μl of the particular lectin solution (3.125–100 pmol/well, serial dilution) for 20 min at 4 °C. At this temperature the metabolism of the cell is down regulated, and energy dependent transport processes are repressed. Consequently, the amount of cell-associated lectin refers basically to cytoadhesion.

Excess of lectin was removed by washing the monolayers twice with 150 μl PBS. Then, 50 μl PBS was added and the mean fluorescence intensity (MFI) of each well was determined using a fluorescence microplate reader (Infinite M200, Tecan, Grödig/Salzburg, Austria). Blanks were prepared accordingly but using PBS instead of the lectin solution and the values obtained were subtracted from all data quoted. Experiments were carried out in quadruplicate.

Single cells were processed immediately after trypsination. 50 μl cell suspension (3.0×10^5 cells) was incubated with 50 μl of a dilution series of the respective lectin in PBS (3.125–100 pmol/assay) for 5 min at 4 °C. Then, 100 μl PBS was added and cells were spun down (1000 rpm, 5 min, 4 °C). The supernatant was discarded and this washing step was repeated twice to remove any unbound lectin. To obtain a suitable single cell suspension, the cells were diluted with 1 ml particle free PBS followed by flow cytometric analysis. In order to estimate the autofluorescence of the cells, control samples with unlabeled cells were included in all experiments and the acquired values were subtracted from all data quoted. Experiments were carried out in triplicate.

2.4. Specificity of the lectin-cell interaction

Specificity of lectin binding was verified by competitive inhibition using the corresponding carbohydrates (Table 1).

Confluent monolayers were washed twice with 150 μl PBS prior to incubation with 100 μl of the complementary carbohydrate in PBS and 50 μl of the corresponding lectin in PBS (25 pmol/well) for 20 min at 4 °C. After a washing step with PBS, cell layers were analysed by fluorimetry after adding 50 μl PBS. For each lectin the amount of inhibitory sugars added is displayed in Table 1.

For single cell experiments, 50 μl cell suspension (3.0×10^5 cells), 100 μl of a dilution series of the lectin-specific carbohydrate and 50 μl of a solution containing 25 pmol lectin were processed as described above.

2.5. Cytoinvasion studies

In order to investigate potential internalisation of lectins, uptake of WGA by ECV304 cells was studied in detail using single cells. In case of PBMEC/C1–2 cells uptake of WGA and additionally DBA was elucidated.

At this, 50 μl cell suspension (3.0×10^5 cells) was incubated with 50 μl of the respective lectin solution (25 pmol WGA or 25 pmol DBA/assay) for 5 min at 4 °C (pulse incubation). Unbound lectin was removed as described above, and cells were further incubated for 0–240 min at 37 °C or 4 °C. As described previously, at 4 °C interaction between the lectin and the cell is limited to binding to the cell surface, whereas at 37 °C cells are metabolically active allowing energy consuming transport processes. At the end of the chase-incubation, MFI values were acquired by flow cytometry. Then, 40 μl monensin solution (2.4 mM in EtOH) was added to the cells followed by a further incubation for 3 min at room temperature. Finally, the MFI was assessed again.

2.6. Flow cytometry

Flow cytometric measurements were carried out on an Epics XL-MCL analytical flow cytometer (Coulter, FL, USA). Data were acquired using a forward versus side scatter gate to detect the single cell population and exclude cell aggregates and debris. Fluorescence emission was detected at 525 nm (10 nm bandwidth)

Table 1
Specificity of the lectins used in the competitive binding assays.

Lectin	MW	Binding specificity	Inhibitory sugar	Sugar [c] in μmol/analysis (PBMEC/C1–2; ECV304)
WGA	36 000	GlcNAc, sialic acid	GlcNAc, chitotriose	0.002–0.063
STL	100 000	Poly-*n*-acetyllactosamine	GlcNAc, chitotriose	0.016–0.25; 0.004–0.125
LCA	49 000	D-Mannose	D-Mannose	2–32; 0.5–16
UEA-I	63 000	Fucα1–2Galβ1–4GlcNAc–	L-Fucose	0.016–0.5
DBA	120 000	GalNAc–	GalNAc	0.25–4; n.d.
PNA	110 000	Galβ13–GalNAc–	Galactosamine	0.016–0.5; 0.031–1

n.d.: not determined.

after excitation at 488 nm. 3000 cells per sample were acquired and for further calculations the mean channel number of the logarithmic fluorescence intensities of individual peaks (MFI) was used. Amplification of the fluorescence signals was adjusted to put the autofluorescence signal of unlabeled cells in the first decade of the four-decade log range. Data analysis was performed using Coulter System II software 3.0.

2.7. Fluorescence microscopy

To confirm binding and uptake of fluorescein-labeled lectins, fluorescence microscopy was used to visualize these processes: ECV304 and PBMEC/C1–2 cells were stained by incubating 50 μl cell suspension (3.0×10^5 cells) with 50 μl of the respective lectin solution (25 pmol WGA/assay for ECV304; 25 pmol WGA/assay and 25 pmol DBA/assay for PBMEC/C1–2) for 5 min at 4 °C. Then, unbound lectin was removed as described above and cells were further incubated for 240 min at 37 °C. Then, cells were washed again and immediately mounted for microscopy without fixation. Control samples were incubated at 4 °C. Images of labeled cells were obtained using a Nikon Eclipse 50i microscope equipped with an EXFO X-Cite 120 fluorescence illumination system. Excitation and emission filter blocks were at 465-495/515-555 for green fluorescence. Fluorescence pictures were acquired at 40× magnification using Lucia G v5.0 software for image evaluation.

2.8. Statistical analysis

Statistical analyses were carried out comparing two means from independent (unpaired) samples (*t*-test) using the Microsoft Excel® integrated analysis tool. *p* values of <0.05 were considered as significant.

3. Results

3.1. Lectin-binding capacity of PBMEC/C1–2 cells

Six plant lectins with distinct carbohydrate specificities were selected to estimate the binding capacity of PBMEC/C1–2 cells and thus to characterize the glycosylation pattern of the cell surface. At this, monolayers were grown to confluence and incubated with the fluorescein-labeled lectins. For comparison of the data obtained, MFI values of each lectin were related to an apparent conjugation number of 1 mol fluorescein per mol lectin. Generally, the amount of cell-bound lectin increases with the amount of lectin added. As depicted in Fig. 1, the lectin binding to monolayers follows the order: WGA > DBA > LCA = STL > PNA > UEA-I. In case of WGA and DBA, a pronounced binding was observed in presence of 6.25 pmol lectin and above with fluorescence intensities in the range from 70.0 ± 3.3 to 1476.8 ± 58.8 MFI (WGA) or from 98.3 ± 15.0 to 1097.7 ± 72.6 MFI (DBA).

Additionally, flow cytometric analyses were performed to estimate the binding to single cells. The histograms revealed homogenous staining of all cells without appearance of unstained subpopulations. Interestingly, the resulting saturation curves

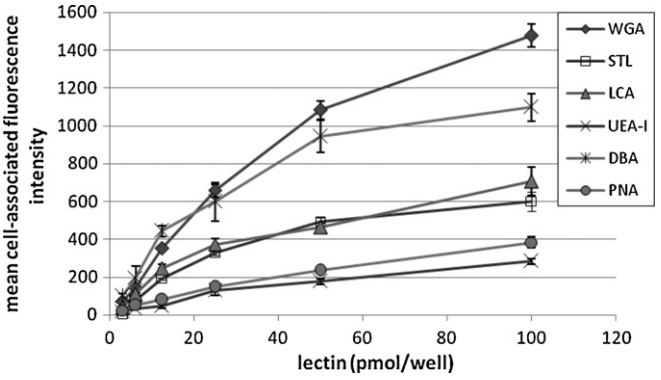

Fig. 1. Saturation curves of lectin binding to PBMEC/C1–2 monolayers with fluorescein-labeled lectins related to an apparent F/P ratio of 1 (mean ± SD, *n* = 4).

(data not shown) were different from those of the monolayer assays. The strongest lectin-interaction with the cell surface was observed with DBA (MFI values up to 20.6 ± 1.4) followed by STL > LCA > WGA > PNA > UEA-I. This ranking of lectin-binding capacity remained stable over the applied concentration range between 3.1 and 100 pmol lectin/analysis and is shown in Fig. 2 at a concentration of 25 pmol. In this figure, the MFI of the lectin with the highest binding capacity was set to 100% and the binding capacities of the other lectins were related to this. Thus, a comparison of the lectin-binding pattern of monolayers and single cells should be possible, which is also depicted in Fig. 2.

3.2. Lectin-binding capacity of ECV304 cells

For ECV304 monolayers, which were cultivated for 4 days, highest binding capacity was assessed for WGA with fluorescence intensities between 63.0 ± 7.7 and 1108.1 ± 65.1 MFI (Fig. 3). In presence of 25 pmol WGA/well the fluorescence intensity was 2.9-, 5.9-, 11.6- or 14.7-fold higher as compared to STL, LCA, UEA-I or PNA, respectively.

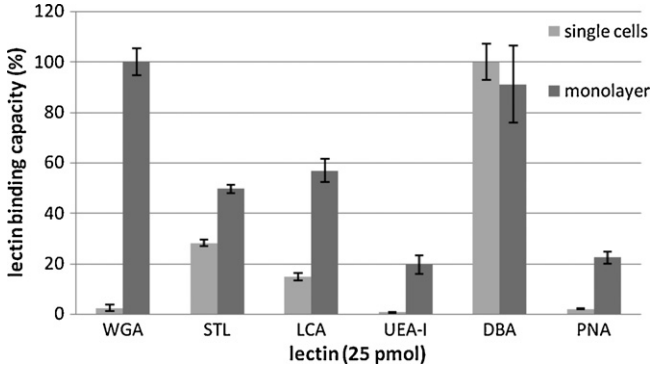

Fig. 2. Comparison of the lectin-binding capacities of single cells and monolayer of PBMEC/C1–2 cells related to the highest binding capacity using a lectin concentration of 25 pmol (mean ± SD, *n* = 3).

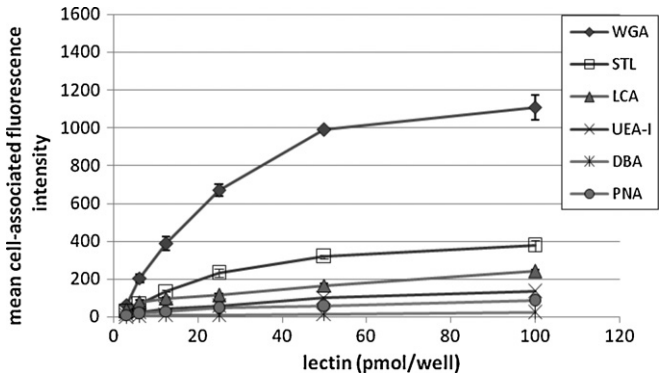

Fig. 3. Saturation curves of lectin binding to ECV304 monolayers grown for 4 days with fluorescein-labeled lectins related to an apparent F/P ratio of 1 (mean ± SD, $n = 4$).

In order to follow alterations in the glycosylation pattern during cultivation, saturation experiments were additionally performed with ECV304 monolayers grown for 14 days. Interestingly, after prolonged cultivation WGA binding was only slightly increased with fluorescence values between 100.5 ± 5.7 and 1374.0 ± 43.6 MFI (data not shown), whereas the binding capacity of the other lectins increased notedly. As exemplified at a concentration of 25 pmol, WGA showed no significant increase between 4 and 14 days cultivation ($p > 0.05$), whereas the binding of all other lectins significantly increased ($p < 0.01$ for STL, LCA, PNA; $p < 0.05$ for UEA-I; Fig. 4). Thus, after 14 days of cultivation, the cell-bound fluorescence intensity of WGA was only 2.2-, 2.8-, 7.0- and 8.4-fold higher as compared to STL, LCA, UEA-I and PNA.

Analyses of single cells led to saturation curves following the same order as for monolayers (data not shown). WGA yielded fluorescence intensities between 0.4 ± 0.1 and 34.5 ± 2.8 MFI followed by STL (0.0 ± 0.0 to 11.8 ± 1.9 MFI) and LCA (0.1 ± 0.0 to 2.9 ± 0.3). Fig. 4 summarizes the lectin-binding capacity at a concentration of 25 pmol/analysis for monolayers and single ECV304 cells. Interestingly, at this concentration LCA possessed a higher binding capacity in comparison to STL (1.4 ± 0.1 MFI as opposed to 0.6 ± 0.2 MFI).

DBA generally yielded very low MFI values scarcely above the autofluorescence of the cells for both, monolayers and single cells.

3.3. Specificity of the lectin-cell interaction

The specificity of the lectin binding was investigated by competitive inhibition using a dilution series of the corresponding carbohydrate and a constant amount of lectin. Depending on the amount of sugar added, the carbohydrate combining site of the lectin is blocked and inhibited from binding to the cell surface. For confluent PBMEC/C1–2 and ECV304 layers, the applied sugar concentrations and the resulting inhibition values are listed in Table 2. These data show that the amount of cell-bound lectin decreases in presence of increasing amounts of the corresponding carbohydrate. Regarding the degree of inhibition, highly specific binding of the respective lectin to cellular structures was determined for ECV304 cells with inhibition values of more than 80% for each individual lectin. In case of PBMEC/C1–2 cells, WGA (93%) and DBA (86%) revealed a highly specific interaction. As the inhibition curves (not shown) are flattening at these percentages, the amount of unspecific binding might be estimated. In case of ECV304 cells, up to 6% of WGA were found to be unspecifically bound, whereas for PBMEC/C1–2 cells the unspecifically bound fraction was at the most about 7% in case of WGA and 14% in case of DBA.

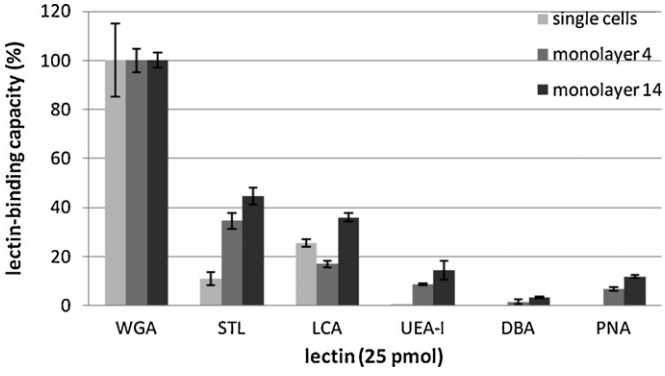

Fig. 4. Comparison of the lectin-binding capacities of single cells and monolayers of ECV304 cells related to the highest binding capacity using a lectin concentration of 25 pmol (mean ± SD, $n = 3$).

However, it has to be considered that there are major differences in the binding behaviour between lectins and their corresponding mono- and oligosaccharide as well as derivatives due to varying affinities. Thus, the calculated specificities are only valid for the respective sugar used and the quoted specificity is assumed to be an asymptotic approximation commonly used in lectin studies to verify that binding to the cells is specific as it can be blocked by increasing amounts of sugar added.

For comparison of the inhibition data between the cell lines, IC_{50} values were calculated from inhibition curves of each lectin and displayed in Table 2. The IC_{50} is defined as the amount of inhibitory sugar which half-inhibits the lectin-cell interaction.

For WGA and PNA no significant differences were observed between the cell lines, whereas the other lectins revealed a stronger affinity to PBMEC/C1–2 than to ECV304 cells.

Specificity of binding was also ascertained for single cells. For both cell lines, a high degree of specific binding was detected for all lectins (data not shown). Interestingly, the estimated specificity of UEA-I with PBMEC/C1–2 single cells was higher than that with monolayers yielding an inhibition curve that leveled off at 95% after addition of 0.5 μmol L-fucose. However, this might also be due to a lower affinity of the interaction between UEA-I and the single cells. The other lectins showed similar inhibition values as compared to the monolayer results. As to ECV304 cells, data similar to monolayer assays were obtained for all lectins with highest inhibition values for STL (92% after addition of 0.125 μmol chitotriose).

3.4. Uptake of WGA and DBA into PBMEC/C1–2 cells

During pulse incubation at 4 °C, WGA was allowed to bind to the cell membrane of PBMEC/C1–2 cells followed by removal of unbound lectin to guarantee identical starting conditions. Then, chase-incubation at 37 °C was started and resulted in a time-dependent decrease of MFI finally yielding a difference of 3.9 ± 0.3 MFI after 240 min as compared to samples incubated at 4 °C for the same time (7.3 ± 0.4 MFI). Upon addition of monensin the reduced MFI could be restored approaching that of the control samples measured immediately after pulse incubation (0 min, 7.0 ± 0.1 MFI). Control samples prepared at 4 °C revealed no considerable differences between MFI values prior to and after monensin addition throughout the incubation time (data not shown).

For DBA, the lectin-cell interaction after pulse incubation at 4 °C resulted in MFI values of 56.3 ± 6.1. At the end of the chase-incubation after 240 min a difference of 33.1 ± 3.6 MFI was detected between samples incubated at 4 °C (60.6 ± 4.7 MFI) and 37 °C (27.5 ± 5.7 MFI), respectively. In contrast to WGA, the addition of monensin did not result in a full recovery of the reduced fluorescence intensities. It only increased from 27.5 ± 5.7 (240 min, 37 °C, without monensin) to 37.1 ± 7.2 (240 min, 37 °C, with monensin). Control samples prepared at 4 °C reacted as described above (data not shown).

Table 2
Competitive inhibition of lectin binding (25 pmol) to confluent PBMEC/C1–2 or ECV304 monolayers by addition of increasing amounts of the complementary carbohydrate.

Lectin + inhibiting sugar	PBMEC/C1–2			ECV304		
	Sugar [c] in μmol/reaction	% inhibition	IC_{50}	Sugar [c] in μmol/reaction	% inhibition	IC_{50}
WGA + chitotriose	0.002	28.19	0.0036	0.002	27.24	0.0034
	0.004	55.90		0.004	59.70	
	0.008	68.55		0.008	64.32	
	0.016	82.41		0.016	82.42	
	0.031	90.33		0.031	88.89	
	0.063	93.03		0.063	94.55	
STL + chitotriose	0.016	48.57	0.018	0.004	42.85	0.006
	0.031	65.16		0.008	61.72	
	0.063	77.95		0.016	74.13	
	0.125	82.11		0.031	85.50	
	0.25	83.32		0.063	91.99	
				0.125	96.79	
LCA + D-mannose	2	41.54	2.8	0.5	26.73	0.9
	4	63.76		1	56.81	
	8	71.19		2	72.43	
	16	71.22		4	83.95	
	32	82.38		8	90.73	
				16	93.12	
UEA-I + L-fucose	0.016	0.23	0.18	0.016	27.92	0.08
	0.031	11.16		0.031	29.17	
	0.063	33.79		0.063	43.13	
	0.125	45.26		0.125	68.77	
	0.25	55.89		0.25	80.24	
	0.5	67.57		0.5	87.34	
DBA + GalNAc	0.25	0.69	0.8	n.d.	n.d.	
	0.5	15.32				
	1	73.82				
	2	83.38				
	4	85.53				
PNA + galactosamine	0.156	16.03	0.14	0.031	25.87	0.14
	0.031	25.26		0.063	41.72	
	0.063	39.60		0.125	47.69	
	0.125	48.77		0.25	69.64	
	0.25	58.74		0.5	74.00	
	0.5	78.65		1	80.66	

n.d.: not determined.

3.5. Uptake of WGA into ECV304 cells

In case of ECV304 cells, membrane-association of WGA after pulse incubation at 4 °C amounted to 54.0 ± 5.9 MFI. During chase-incubation, a difference of 25.8 ± 1.2 MFI was assessed after 240 min between samples incubated at 4 °C (53.8 ± 3.7 MFI) and 37 °C (27.9 ± 1.1 MFI). Again, reduced MFI values could be restored upon addition of monensin and control samples prepared at 4 °C revealed no differences of MFI values prior to and after monensin addition (Fig. 5).

3.6. Fluorescence microscopy

For both cell lines, the images acquired after incubation at 4 °C confirmed that the lectins bind exclusively to the surface of the cells as indicated by a fluorescent ring encircling the cell, when the focus was set to the middle of the cells. Incubation at 37 °C gave decisive hints towards intracellular enrichment for WGA in case of ECV304 cells and for WGA as well as DBA in case of PBMEC/C1–2 cells, as the fluorescence was predominantly located within the cell (Fig. 6).

4. Discussion

In this study different plant lectins with distinct sugar specificities were applied to the human cell line ECV304 and the porcine cell line PBMEC/C1–2 in order to elucidate the carbohydrate composition of the glycocalyx and to evaluate the scale of lectin-cell interactions for lectin-mediated targeting. Since precise determination of the total amount of non-specific binding by competitive inhibition assays is sometimes not feasible and both, specific and unspecific binding will contribute to the lectin-interaction in vivo when applied for drug delivery purposes, total binding of the lectin was assumed to be most appropriate.

Cell lines ECV304 and PBMEC/C1–2 were chosen for these studies, because several reports revealed the suitability of both cell lines for BBB studies (Easton and Abbott, 2002; Kuhlmann et al., 2008,

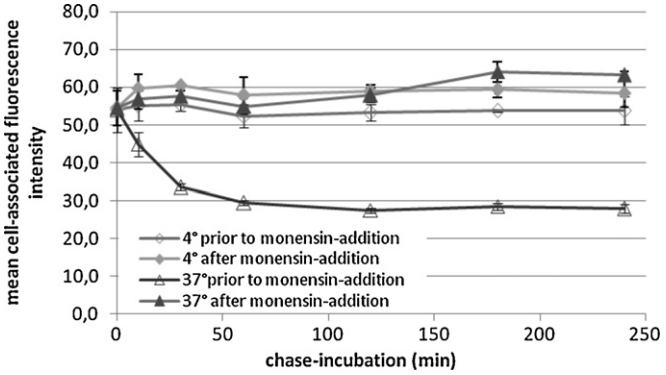

Fig. 5. Mean fluorescence intensities of ECV304 cells loaded with 25 pmol WGA prior and after addition of monensin during incubation at 4 and 37 °C by time up to 4 h (mean ± SD, $n = 3$).

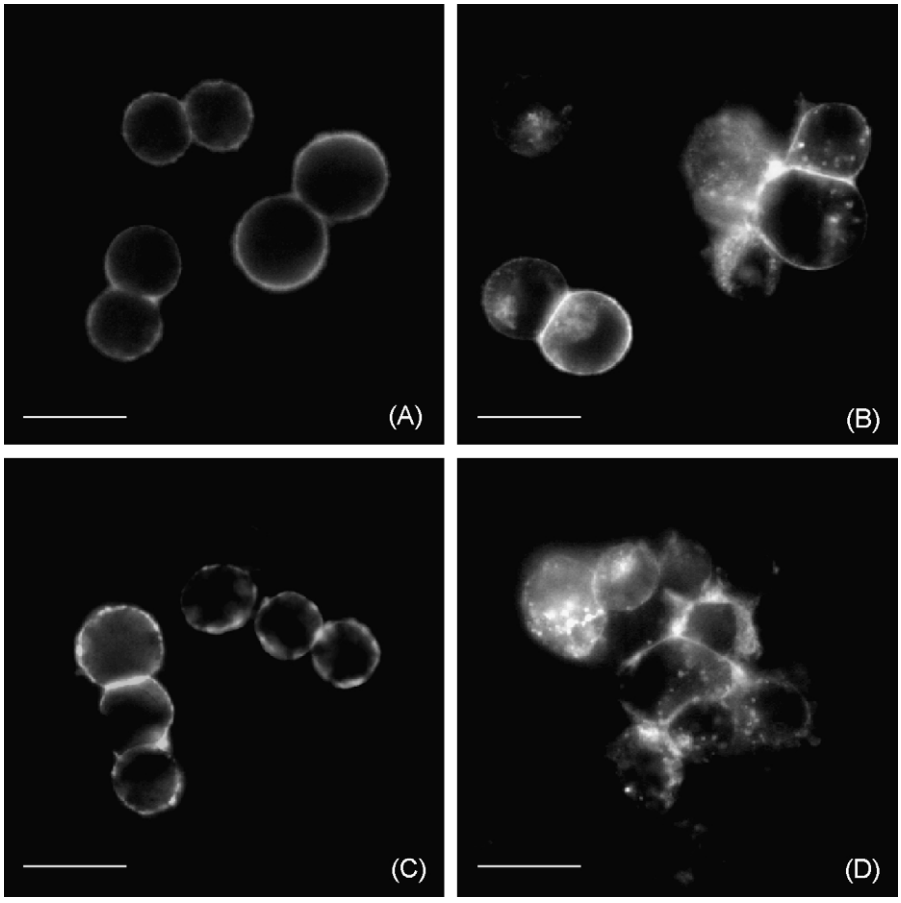

Fig. 6. Fluorescence microscopy images of ECV304 cells incubated with fluorescein-labeled WGA (25 pmol) for 240 min at 4 °C (A) and 37 °C (B) and PBMEC/C1–2 cells incubated with fluorescein-labeled DBA (25 pmol) for 240 min at 4 °C (C) and 37 °C (D). Scale bar represents 20 μm.

2009; Krämer et al., 2002; Suda et al., 2001; Teifel and Friedl, 1996; Vanier et al., 2004, 2006). In this context, one of the most important properties of BBB in vitro models is the inducibility of specific BBB features by astrocytes, pericytes or specific components of the basement membrane as laminin. At this, both cell lines significantly respond to astrocytic or glioma signals. For example, BBB characteristics as TEER, expression of tight junction molecules, transferrin receptor, P-glycoprotein (P-gP), glucose transporter GLUT-1 and gamma glutamyl transpeptidase were upregulated by astrocytes, rat C6 glioma or their soluble factors in ECV304 or PBMEC/C1–2 (Dolman et al., 1998; Kuchler-Bopp et al., 1999; Hurst and Fritz, 1996; Easton and Abbott, 2002; Neuhaus et al., 2008a,b). In case of ECV304 cells, it has to be alluded that doubt has been raised over the use for BBB studies and whether these cells are endothelial (Brown et al., 2000; Drexler et al., 2002). However, several studies have shown that BBB properties were inducible when ECV304 from ECACC were co-cultured with astrocytes or glioma cell line C6 (Hurst and Fritz, 1996; Easton and Abbott, 2002; Kuchler-Bopp et al., 1999; Dolman et al., 1998; Neuhaus et al., 2008b). Since inducibility of BBB properties is one of the most important features for BBB models, we applied ECV304 cells from ECACC for our studies. Furthermore, it was shown that ECV304 were suitable for TEER dependent transport studies (Neuhaus et al., 2008c). In summary, both cell lines exhibit typical BBB properties making them qualified models for the presented studies.

Ongoing from the lectin-binding pattern of PBMEC/C1–2 monolayers the detectable carbohydrate composition can be characterized as follows: *N*-acetyl-D-glucosamine and sialic acid residues as corresponding carbohydrates of WGA seem to be most prevailing and accessible. The ubiquitous presence of GlcNAc moieties in the glycocalyx of cells makes it rather difficult to specify the target structure, possible binding sites could be provided by *N*-linked glycans of the hybrid-type (Yamamoto et al., 1981). High-mannose-type *N*-glycans can be identified via binding of LCA (Akama et al., 2006), and turned out to be of medium presence. The high binding of DBA to PBMEC/C1–2 cells accounts for the presence of *N*-acetyl-D-galactosamine residues, which are linked to proteins in the first step of the *O*-glycosylation pathway. The GalNAc-epitope can further be converted to the core 1 structure Galβ1–GalNAc– and extended to Fucα1–2Galβ1–4GlcNAc-residues, providing possible binding sites for PNA and UEA-I, respectively (Galvan et al., 1998). However, these binding sites were found to be less abundant in PBMEC/C1–2 monolayers. In general, findings are in accordance to Fischer and Kissel (Fischer and Kissel, 2001) who stained primary capillary endothelial cells from porcine brain with lectins and detected a strong affinity for WGA, followed by DBA. However, no affinity was found for PNA in this study, whereas Plendl et al. showed labeling of endothelial cells isolated from the brain of fetal pigs (Plendl et al., 1996). Besides WGA, UEA-I was proposed for the characterization of porcine capillary endothelium (Fischer and Kissel, 2001). Nevertheless, the marginal occurrence of UEA-I binding sites on PBMEC/C1–2 cells was quite predictable as Teifel and Friedl did not detect UEA-I binding of this cell line using a different fixation method and lower concentrations (Teifel and Friedl, 1996). Previous studies reported alterations in the sugar composition during BBB development (Vorbrodt et al., 1986; Nico et al., 1998) and a different lectin-binding pattern after changes in the barrier function (Nishida et al., 1986; Szumanska and Albrecht, 1997). For PBMEC/C1–2 cells these possible changes in the glyocalyx composition due to the influence of age and differentiation could not

be assessed as the cells start to detach within 4 days after reaching confluence (Neuhaus et al., 2008a). Therefore, lectin-binding studies were only carried out on day 4 after seeding.

Experiments with single cells resulted in an apparent predominance of *N*-acetyl-D-galactosamine structures (DBA). Interestingly, *N*-acetyl-D-glucosamine and sialic acid residues corresponding to WGA-binding were found to be less abundant whereas the lectin-binding capacities of the other lectins remained similar. These differences might be due to a loss of cellular polarity or the use of trypsin prior to the single cell experiments.

Comparing the results of monolayer and single cell studies, cultivation of PBMEC/C1–2 monolayers appears more appropriate for lectin-interaction studies as the lectin-binding pattern on monolayers better correspond to primary endothelial cells and cortical brain sections. Ongoing from this good correlation, this cell line seems to be suitable as an *in vitro* model of the BBB for lectin-mediated drug delivery studies.

Lectin-binding studies using ECV304 monolayers cultivated for 4 days resulted in a glycosylation pattern as follows: *N*-acetyl-D-glucosamine and sialic acid moieties as detected by WGA are highly accessible and therefore probably most abundant. According to their detection the other accessible sugar residues follow the order: Poly-*n*-acetyllactosamine (STL) > D-mannose (LCA) > Fucα1–2Galβ1–4GlcNAc (UEA-I) > Galβ1–GalNAc– (PNA) and *N*-acetyl-D-galactosamine (DBA). Since ECV304 cells differentiate over 2 weeks (Easton and Abbott, 2002; Neuhaus et al., 2008a), ECV304 monolayers were also cultivated for 14 days. Results revealed significant changes of the amount of the respective lectin-binding sites except for *N*-acetyl-D-glucosamine and sialic acid residues reflected by WGA-interaction. Increase of UEA-I binding during cultivation, which was previously found and described as an endothelial cell feature of ECV304 cells (Kiessling et al., 1999), underlines once more the endothelial character of this cell line and its utility as an BBB *in vitro* model. No changes were observed with respect to the ranking of the lectin-binding capacities. As above, highest binding rates were detected for WGA.

Single cell assays with ECV304 cells revealed a lectin-binding ranking similar to that of monolayer studies. However, there is only a limited number of accessible binding sites for UEA-I and PNA in comparison to monolayers, so that cultivation of ECV304 monolayers seems more appropriate.

Comparing the monolayer studies after 4 days in culture, both cell lines yielded the highest binding capacity for WGA together with a high binding specificity. The almost complete absence of DBA binding sites on ECV304 cells as opposed to PBMEC/C1–2 cells may be due to the human origin of ECV304 cells as *N*-acetyl-galactosamine was also scarcely detected in former studies on other human cell lines (Gabor et al., 1998; Gabor et al., 2001; Wirth et al., 2002; Toegel et al., 2007). The binding of the remaining lectins to PBMEC/C1–2 cells was notedly higher than to ECV304 cells.

For lectin-mediated drug delivery not only binding of the targeter but also uptake is desirable. Ongoing from the characterization of the sugar composition of the two cell lines, WGA and DBA seem to be suitable for further investigations in case of porcine PBMEC/C1–2 cells, whereas only WGA seems to be a promising candidate lectin for human ECV304 cells. For both cell lines internalisation of WGA could be demonstrated qualitatively via fluorescence microscopy as exemplified for ECV304 in Fig. 6A and B. Ongoing from these results, enrichment of WGA within acidic compartments of the cell was confirmed using monensin. Since the quantum yield of fluorescein is known to be reduced at acidic pH and addition of monensin can compensate the pH-gradient between acidic compartments and the cytoplasm, the decrease of MFI during chase-incubation at 37 °C associated with a full recovery of the MFI values after addition of monensin points to lysosomal accumulation of the internalized lectin. As no fluorescent WGA was detectable in the supernatant, it was even possible to calculate the fraction of WGA taken up into the cell (Gabor et al., 2001). In case of PBMEC/C1–2 cells, about 30% of initially cell bound lectin were internalized within 10 min, at the end of the chase-incubation about 60% were accumulated in acidic compartments. For ECV304 cells, uptake of WGA was almost similar (20% after 10 min and 55% after 240 min). Furthermore, the potential of DBA as targeting vehicle to PBMEC/C1–2 cells could be assessed. Similar to WGA, MFI decreased continuously during chase-incubation from 56.3 to 27.5 at 37 °C. Interestingly, addition of monensin did not result in total recovery of the initial values. Therefore, possible detachment of initially membrane-bound lectin was considered, but no fluorescent DBA was detectable in the supernatant of the samples. Moreover, lysis of the cell pellets resulted in similar MFI values for both setups (4° and 37°). In addition, fluorescence microscopy also revealed uptake of DBA (Fig. 6C and D). Hence, in case of DBA, the quenching effects might result from an accumulation and constriction of the target vehicle in different, not exclusively acidic vesicular compartments of the cell.

All in all, evaluation of the interaction between lectins and the glycocalyx of BBB mimicking cells demonstrated potential applicability of lectins as a tool to improve drug transport across the BBB. For both cell lines, accessible lectin-binding sites were detected and the interaction of certain lectins is promising and characterized by high binding strength and specificity. In general, WGA seems to be a suitable candidate for lectin-grafted drug-delivery systems in case of human ECV304 cells, whereas WGA and DBA seem to be promising candidate lectins for porcine PBMEC/C1–2 cells. As similar results to primary cells and brain sections were obtained, both cell lines can serve as models for lectin-interaction studies in BBB research, preferentially after cultivation of monolayers.

References

Akama, T.O., Nakagawa, H., Wong, N.K., Sutton-Smith, M., Dell, A., Morris, H.R., Nakayama, J., Nishimura, S.I., Pai, A., Moremen, K.W., Marth, J.D., Fukuda, M.N., 2006. Essential and mutually compensatory roles of α-mannosidase II and α-mannosidase IIx in *N*-glycan processing in vivo in mice. PNAS 103, 8983–8988.

Benda, P., Lightbody, J., Sato, G., Levine, L., Sweet, W., 1968. Differential rat glial cell strain in tissue culture. Science 161, 370–371.

Bies, C., Lehr, C.M., Woodley, J.F., 2004. Lectin-mediated drug targeting: history and applications. Adv. Drug. Del. Rev. 56, 425–435.

Brown, J., Reading, S.J., Jones, S., Fitchett, C.J., Howl, J., Martin, A., Longland, C.L., Michelangeli, F., Dubrova, Y.E., Brown, C.A., 2000. Critical evaluation of ECV304 as a human endothelial cell model defined by genetic analysis and functional responses: a comparison with the human bladder cancer derived epithelial cell line T24/83. Lab. Invest. 80, 37–45.

Cucullo, L., Aumayr, B., Rapp, E., Janigro, D., 2005. Drug delivery and in vitro models of the blood–brain barrier. Curr. Opin. Drug. Discov. Dev. 8, 89–99.

Dolman, D.E.M., Anderson, P., Rollison, C., Abbott, N.J., 1998. Characterisation of a new in vitro model of the blood–brain barrier (BBB). J. Physiol. 505, 56–57.

Drexler, H.G., Quentmeier, H., Dirks, W.G., MacLeod, R.A., 2002. Bladder carcinoma cell line ECV304 is not a model system for endothelial cells. In Vitro Cell. Dev. Biol. Anim. 38, 185–186.

Easton, A.S., Abbott, N.J., 2002. Bradykinin increases permeability by calcium and 5-lipoxygenase in ECV304/C6 cell culture model of the blood–brain barrier. Brain Res. 953, 157–169.

Fatehi, M.I., Gerhart, D.Z., Myers, T.G., Drewes, L.R., 1987. Characterization of the blood–brain barrier: glycoconjugate receptors of 14 lectins in canine brain, cultured endothelial cells, and blotted membrane proteins. Brain Res. 415, 30–39.

Fischer, D, Kissel, T., 2001. Histochemical characterization of primary capillary endothelial cells from porcine brains using monoclonal antibodies and fluorescein isothiocyanate-labelled lectins: implications for drug delivery. Eur. J. Pharm. Biopharm. 52, 1–11.

Gabor, F., Wirth, M., 2003. Lectin-mediated drug delivery: fundamentals and perspectives. STP Pharma Sci. 13, 3–16.

Gabor, F., Stangl, M., Wirth, M., 1998. Lectin-mediated bioadhesion: binding characteristics of plant lectins on the enterocyte-like cell lines, Caco-2, HT-29 and HCT-8. J. Control. Rel. 55, 131–142.

Gabor, F., Klausegger, U., Wirth, M., 2001. The interaction between wheat germ agglutinin and other plant lectins with prostate cancer cells Du-145. Int. J. Pharm. 221, 35–47.

Galvan, M., Murali-Krishna, K., Ming, L.L., Baum, L., Ahmed, R., 1998. Alterations in cell surface carbohydrates on T cells from virally infected mice can distinguish effector/memory CD8+ T cells from naïve cells. J. Immunol. 161, 641–648.

Garberg, P., Ball, M., Borg, N., Cecchelli, R., Fenart, L., Hurst, R.D., Lindmark, T., Mabondzo, A., Nilsson, J.E., Raub, T.J., Stanimirovic, D., Terasaki, T., Oberg, J.O., Osterberg, T., 2005. In vitro models for the blood–brain barrier. Toxicol. In Vitro 19, 299–334.

Hurst, R.D., Fritz, I.B., 1996. Properties of an immortalized vascular endothelial/glioma cell co-culture model of the blood–brain barrier. J. Cell. Physiol. 167, 81–88.

Janzer, R.C., Raff, M.C., 1987. Astrocytes induce blood–brain barrier properties in endothelial cells. Nature 325, 253–257.

Joo, F., 1996. Endothelial cells of the brain and other organ systems: some similarities and differences. Prog. Neurobiol. 48, 255–273.

Kiessling, F., Kartenbeck, J., Haller, C., 1999. Cell-cell contacts in the human cell line ECV304 exhibit both endothelial and epithelial characteristics. Cell Tissue Res. 297, 131–140.

Krämer, S.D., Schütz, Y.B., Wunderli-Allenspach, H., Abbott, N.J., Begley, D.J., 2002. Lipids in blood–brain barrier models in vitro II: Influence of glial cells on lipid classes and lipid fatty acids. In Vitro Cell. Dev. Biol. Anim. 38, 566–571.

Kuchler-Bopp, S., Delaunoy, J.P., Artault, J.C., Zaepfel, M., Dietrich, J.B., 1999. Astrocytes induce several blood–brain barrier properties in non-neural endothelial cell. Neuroreport 10, 1347–1353.

Kuhlmann, C.R., Gerigk, M., Bender, B., Closhen, D., Lessmann, V., Luhmann, H.J., 2008. Fluvastatin prevents glutamate-induced blood–brain-barrier disruption in vitro. Life Sci. 82, 1281–1287.

Kuhlmann, C.R., Zehendner, C.M., Gerigk, M., Closhen, D., Bender, B., Friedl, P., Luhmann, H.J., 2009. MK801 blocks hypoxic blood–brain-barrier disruption and leukocyte adhesion. Neurosci. Lett. 449, 168–172.

Lehr, C.M., 2000. Lectin-mediated drug delivery: the second generation of bioadhesives. J. Control. Release 65, 19–29.

Naeem, A., Saleemuddin, M., Khan, R.H., 2007. Glycoprotein targeting and other applications of lectins in biotechnology. Curr. Prot. Pept. Sci. 8, 261–271.

Neuhaus, W., Plattner, V.E., Wirth, M., Germann, B., Lachmann, B., Gabor, F., Noe, C.R., 2008a. Validation of in vitro cell culture models of the blood–brain barrier: tightness characterization of two promising cell lines. J. Pharm. Sci. 97, 5158–5175.

Neuhaus, W., Wirth, M., Plattner, V.E., Germann, B., Gabor, F., Noe, C.R., 2008b. Expression of Claudin-1, Claudin-3 and Claudin-5 in human blood–brain barrier mimicking cell line ECV304 is inducible by glioma-conditioned media. Neurosci. Lett. 446, 59–64.

Neuhaus, W., Trauner, G., Gruber, D., Oelzant, S., Klepal, W., Kopp, B., Noe, C.R., 2008c. Transport of a $GABA_A$-receptor modulator and its derivatives derived from *Valeriana officinalis* L. s.l. across an in vitro cell culture model of the blood–brain barrier. Planta Med. 74, 1338–1344.

Nico, B., Quondamatteo, F., Ribatti, D., Bertossi, M., Russo, G., Herken, R., Roncali, L., 1998. Ultrastructural localization of lectin binding sites in the developing brain microvasculature. Anat. Embryol. 197, 305–315.

Nishida, S., Akai, F., Hiruma, S., Maeda, M., Tanji, K., Hashimoto, S., 1986. Experimental study of WGA binding on the endothelial cell surface in cerebral ischemia. Histol. Histopathol. 1, 69–74.

Plendl, J., Neumuller, C., Vollmar, A., Auerbach, R., Sinowatz, F., 1996. Isolation and characterization of endothelial cells from different organs of fetal pigs. Anat. Embryol. 194, 445–456.

Suda, K., Rothen-Rutishauser, B., Günthert, M., Wunderli-Allenspach, H., 2001. Phenotypic characterization of human umbivilical vein endothelial (ECV304) and urinary carcinoma (T24) cells: endothelial versus epithelial features. In Vitro Cell. Dev. Biol. Anim. 37, 505–514.

Szumanska, G., Albrecht, J., 1997. Lectin histochemistry of the rat brain following thioacetamide-induced hepatic failure. Mol. Chem. Neuropathol. 32, 163–177.

Takahashi, K., Sawasaki, Y., Hata, J.J., Mukai, K., Goto, T., 1990. Spontaneous transformation and immortalization of human endothelial cells. In Vitro Cell. Dev. Biol. 25, 265–274.

Teifel, M., Friedl, P., 1996. Establishment of the permanent microvascular endothelial cell line PBMEC/C1–2 from porcine brains. Exp. Cell. Res. 228, 50–57.

Toegel, S., Harrer, N., Plattner, V.E., Unger, F.M., Viernstein, H., Goldring, M.B., Gabor, F., Wirth, M., 2007. Lectin binding studies on C-28/I2 and T/C-28a2 chondrocytes provide a basis for new tissue engineering and drug delivery perspectives in cartilage research. J. Control. Rel. 117, 121–129.

Vanier, G., Segura, M., Friedl, P., Lacouture, S., Gottschalk, M., 2004. Invasion of porcine brain microvascular endothelial cells by *Streptococcus suis* serotype 2. Infect. Immun. 72, 1441–1449.

Vanier, G., Szczotka, A., Friedl, P., Lacouture, S., Jacques, M., Gottschalk, M., 2006. Haemophilus parasuis invades porcine brain microvascular endothelial cells. Microbiology 152, 135–142.

Vorbrodt, A.W., Lossinsky, A.S., Dobrogowska, D.H., Wisniewski, H.M., 1986. Distribution of anionic sites and glycoconjugates on the endothelial surfaces of the developing blood–brain barrier. Brain Res. 29, 69–79.

Wirth, M., Kneuer, C., Lehr, C.M., Gabor, F., 2002. Studying cellular binding and uptake of bioadhesive lectins. In: Lehr, C.M. (Ed.), Cell Culture Models of Biological Barriers. Taylor and Francis, London/New York, pp. 62–93.

Yamamoto, K., Tsuji, T., Matsumoto, I., Osawa, T., 1981. Structural requirements for the binding of oligosaccharides and glycopeptides to immobilized wheat germ agglutinin. Biochemistry 20, 5894–5899.